

Ultra-compact structure with snap-through behaviour for multi-stability

Ruta STANKEVICIUTE*, Jun SATO

*Graduate School of Frontier Sciences, The University of Tokyo
Chiba, Kashiwa, Kashiwanoha, 5-1-5
ruta@g.ecc.o-tokyo.ac.jp

Abstract

Lightweight structures composed of thin members tend to bend rather than stretch. This characteristic makes them susceptible to elastic instability, commonly observed in structural engineering as a failure of the structure. However, in nature, snap-through instability is used to transform structures from one equilibrium stage to another without damaging the structure and achieving multi-stability. Furthermore, the bifurcation point, which defines at which load structure passes through the instability phase, can be highly influenced by geometry instead of an increase in the mass of the materials. Therefore, in this paper, a novel design approach for deployable structures is proposed, where snap-through behaviour is utilized to increase the structure's load-bearing capacity and reduce the material to the minimum, creating an ultra-compact structure. The skeleton of the structure was developed by bundling flexible members together and creating buckled regions replicating snap-through geometry observed in nature. In this way, localized stiffness was created throughout the structure, enabling the construction of a meter-scale skeleton by means of physical prototyping and 3d printing only. However, to enhance the skeleton's ability to support the weight of the membrane, the skeleton was optimized using eigenvalue buckling analysis in conjunction with an evolutionary solver. This study presents a comprehensive methodology for the design, fabrication, analysis, and optimization of ultra-compact structures.

Keywords: ultra-compact, deployable, snap-through, eigenvalue buckling analysis, multi-stability.

1. Introduction

The field of deployable structures has captivated scientists, engineers, and architects for decades, tracing its roots to a range of disciplines, including aerospace engineering, architecture, and materials science. The allure of deployable structures lies in their multifaceted applicability—ranging from satellite booms to emergency shelters.

While not always deployable, ultra-compact structures can be best described as a specialized subset within the larger field of deployable structures. These structures are engineered to achieve extreme levels of compactness, often characterized by a high ratio of deployed-to-packed volume. However, in the pursuit of ultra-compactness, one of the most critical challenges is ensuring the vulnerability to elastic instability, that can manifest in multiple ways, from local deformations to global structural failures. However, snap-through buckling offers an intriguing solution to the challenge of elastic instability. Snap-through buckling is a non-linear instability phenomenon that involves a sudden, rapid transition from one stable equilibrium state to another when subjected to an external load or perturbation.

One way to use snap-through buckling is to employ the phenomenon to design multi-stable structures capable of maintaining multiple stable equilibrium configurations. This characteristic has applications in deployable structures, where a single structure can adapt to multiple forms and functions. While there are examples of metre-scale snap-through employing structures, the focus remains on origami structures

[1][2]; notably, the focus on curved geometry remains confined to small scale metamaterials [3] and micro-robotics [4]. In nature, however, while some snap-through geometries are origami-like [5], curved geometries prevail [6]. Additionally, through bending of thin elastic elements, the stiffness can be tuned, reaching maximum stiffness just before the snap-through event, as seen in a twisting and rotating beak of a hummingbird [7].

Therefore, this study focuses on using curved snap-through geometries, similar to those found in nature, to harness stiffening properties of bend-active elements. This way, localized stiffening can be created to enhance load-bearing capacity. By enhancing stiffness through geometry and minimizing material use, an ultra-compact structure is proposed.

2. Method basis

2.1. Stiffening of thin elastic elements

The bifurcation point, or the critical load, for snap-through buckling can be highly influenced by the degree of curvature of the structural members, which can result in a higher load-bearing capacity of the structure without an increase in the mass of the materials. Snap-through behaviour triggers a state of high stiffness in the post-snap-through stage, resulting in a substantial increase in stiffness by several orders of magnitude [8]. This stiffness can be easily manipulated by adjusting the snap-through prone geometry, achieving tuneable stiffness [9].

Conventional pre-shaped beams, renowned for their substantial load-bearing capacity, exhibit a dual behaviour of bending and buckling under axial compression. This simple yet impactful behaviour can prompt reversible and homogeneous pattern transformations within metamaterials composed of regular arrays of elastic beams, contributing to structural stiffening [10]. Moreover, the modal nudging method can tailor the post-buckling behaviour by seeding a post-buckling response over potential alternatives [11]. The concept of a membrane-restrained column, where the membrane prevents external deformation under vertical load, can be another alternative for creating buckled regions within the structure. This restraint leads to a significantly higher buckling load than individual struts. [12] However, while bundling the force-active members, the membrane can be replaced with regions defined by joined buckled elements, creating localized variation in stiffness and deflection [13].

With bundled end-points, strength and stiffness are concentrated at the fixed bundled trunks. Therefore, employing localized bundling of slender rods is proposed, integrating both compression and tensioned rods to replicate the concave and convex shapes inherent in snap-through mechanisms observed in nature. The sliding or umbrella mechanisms exhibit the potential to work for compressing members. Fixing one end of an elastic rod while sliding another end along rectilinear support or guide allows for element buckling, further enabling the fine-tuning of buckled element stiffness by adjusting the sliding joint's position.

2.2 Efficient packing

However, to find the most efficient packing mechanics, compact structures were studied. Typically, deployable structures are designed for storage and transportation efficiency. Therefore, the aerospace sector is a primary driver of advanced research in this field, notably for meter-scale deployable structures.

The highest 100:1 deployment ratio, can be achieved with coiled flexible rod structures and wrapped foldable membranes [14][15], being the most compact deployable mechanics. The coiling allows for a highly compact initial state. At the same time, the material properties and geometry of the rods permit them to extend to several times their initial length, thereby maximizing the deployment ratio.

Thus, the rod structure is proposed as the cornerstone of the method, capitalizing on its coiling capacity for high deplorability ratios and the inherent ability of the umbrella mechanism to facilitate buckled geometry through sliding joints. This choice establishes the fundamental framework for the approach.

3. Design and fabrication

3.1 Container and materials

The Japanese toys known as gacha are sold in vending machines that dispense a random toy in a capsule - the adventure aspect inspired to choose gacha as a vessel for an ultra-compact structure. By packing an average one-person tent into a 7cm gacha capsule, the most common size for larger, 500 yen gachapon machines, a 6000:1 deployment ratio can be achieved.

However, the spherical shape invites complications, with intersecting coiling paths and variable radius due to the nature of the form. Therefore, the gacha capsule design evolves from the conventional spherical form to a cylindrical shape. (fig. 1 (a)). The proposed form inherently offers a consistent radius across its entire exterior surface. A helix compartment running along the side of the cylinder was designed, enabling the structural members to be securely coiled, while the internal compartment of the cylinder is designed to accommodate the structure's exterior membrane. Furthermore, the cylinder's form proves more aligned with transportation and storage logistics, as seen in scenarios like space shuttle transfers.

The Carbon Reinforced Polymer (CRP) rods were an ideal option for this project for their high strength-to-weight ratio and high modulus of elasticity. The inner radius of the helix compartment (R_{min}) is 22.5mm, and can be used to determine the radius (r) of the rod when the yield strain of the material (ϵ_{max}) is known using this formula [16]:

$$r = R_{min} \times \epsilon_{max} \quad (1)$$

The T300 class carbon rods with $\epsilon_{max} = 1.5\%$ were used. Therefore, the radius for the rods comes to be $r = 0.3375\text{mm}$. or $d = 0.675\text{mm}$. From the rods available in the market, 0.5mm diameter carbon rods were chosen, matching closest to the calculation. The rod's thin diameter allows it to be coiled and stored inside a gacha capsule while still providing enough strength when building a 1:1 scale mock-up. For the structure's membrane, super organza was chosen, which weighs only 5g/m^2 at its thinnest configuration, making it one of the lightest materials in the world. It is an ultra-thin fabric composed of very fine seven-denier polyester organza threads. In one gacha capsule, 4m^2 of organza can be packed, sufficient to cover a one-person tent (fig. 1(b)).

3.2 Deployment system

One of the fundamental rules is the alignment of all members in one direction when packed. This arrangement allows the members to be bundled together and coiled. Additionally, the structure must contract in length so the members can fit in a helix on the exterior surface of the cylinder gacha capsule compartment. The length of the structure can be adjusted by implementing the sliding joints that can move along the connected members. Sliding joints were designed so that they could bundle 2 to 7 rods at the same time to reduce the length of the structure to the minimum. However, in some cases, when members cannot be aligned, connectors are used instead of sliding joints, which can be easily disconnected. The joints and connectors were printed using transparent resin to create a seamless, almost invisible appearance, enhancing the structure's overall aesthetic (fig. 1(c)).

Exploring the membrane deployment mechanism, it was decided to use base tensioning, where the structure's foundation is tensioned by fixing legs to the foundation or ground membrane, as commonly seen in tents. The outer membrane can be secured with hooks, making the process more flexible.



Figure 1: A – Cylindric container, B - material packed in a 7cm diameter gacha capsule, C - 3D printed parts.

3.3 Snap-through module

The design process of the structure began by designing tuneable snap-through behaviour in a structure. Building upon the methodological foundation outlined in the previous section, the method used in the design involved the strategic bundling of skeleton elements to define snap-through capable geometry (fig. 2(a)). By manipulating the sliding joints to compress specific rods and introduce tension to others, snapping planes were created, which could be adjusted by sliding the joints, regulating tension and compression (fig. 2(b)).

Through the integration of bundled structural elements and manipulation of localized stiffness and deflection, snap-through behaviour was successfully realized. After joining snapping planes together, a snap-through module was established (fig 2(c)), which exhibited multi-stable behaviour (fig. 2(d1-2)). The structure's interior space could be changed drastically through snapping events, transitioning from low and wide configuration to high and narrow, suggesting possibilities for transformable space.

Prototyping in a 1:1 scale allowed for a more accurate assessment of the modules' structural integrity, functionality, and ability to exhibit snap-through behaviour in a real-world context.

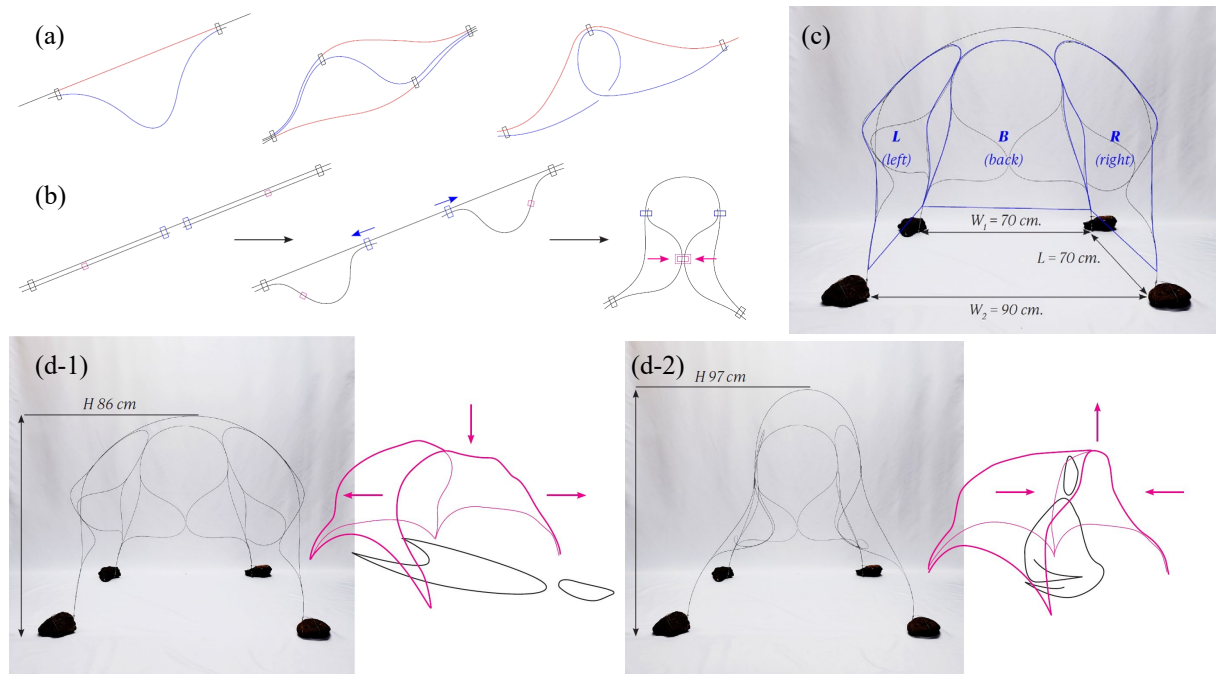


Figure 2: A – Bundling of the slender elements localizing stiffness (red tension, blue compression), B - creating snapping planes by sliding joints to buckle elements and connecting two buckled elements to create snap-through plane, C - Snap-through module with highlighted snap-through planes, D - 1:1 scale snap-through module state 1: sleeping mode (L and R planes snapped outwards) and 2: sitting mode (L and R planes snapped inwards)

4. Analysis and optimization

The limitation of the physical model study in a 1:1 scale using extremely slender elements is the complexity of the structure's behaviour. After applying organza, the structure becomes unstable. Therefore, a computational tool for analysis and optimization was necessary to reconfigure the snap-through module to support the membrane.

4.1 Generating the skeleton

Initially, the structural footprint is defined by a layer of four curves. These curves determine the four distinct planes of the structure: $\{*:0\}$, $\{*:1\}$, $\{*:2\}$, and $\{*:3\}$, which can be twisted and aligned in one direction, following the rules of the deployment (fig.3 (a)). At the same time, another boundary condition is set so that the individual members do not exceed the 2m length limit to facilitate packing the structure into the capsule.

The four primary curves are subdivided into 23 parts, with 24 points each, which serve as the basis for the vertices of subsequent curve layers within the structure. The starting and ending points for these new curves, representing the sliding joints' locations. The lengths of the new curves for the structure's subsequent layers are selected to be between 1 and 2 meters length structural members. To establish snapping planes, connectors are utilized. The starting and ending points for these connector lines are selected along the existing curves (fig.3 (b)).

In the chosen configuration for optimization start (fig. 3 (c-1)), a maximum of 16 curves is generated, with four curves allocated per plane. Similarly, up to 16 connectors can be established. Although the physical model could be recreated with fewer elements and connectors (fig. 3 (c-2)), the freedom to transform the structure was essential for the optimization purposes.

4.2 Pathway analysis set-up

The primary objective of the pathway analysis is to augment physical behaviour to the generated curves and acquire the final geometry of the skeleton (fig. 3(d)). The analysis was built using Kangaroo physics plug-in – an interactive physics engine that reaches set goals using a form of dynamic relaxation. The Kangaroo physics components are used to set up goals for the analysis while Kangaroo solvers run the simulation and provide the result.

The 'Rod' component was employed to represent carbon rods, as this component can simulate the bending behaviour of the elements. For simulating the joints and legs of the structure, an 'Angle' component was utilized. By setting the angle to 0 degrees in the component, all elements are forced into alignment, consistent with observations from the physical model. In terms of connectors, a 'Length' component was employed. When the length of the connector line is set to zero, it enforces a joining of the corresponding points of the structure, effectively simulating the role of connectors in the physical model. Finally, a 'Load' component was incorporated to simulate the weight of the structure. For the solver, the Kangaroo zombie solver was employed, with threshold set at $1.0e-10$, the tolerance at 0.00001, and the maximum number of iterations was capped at 5000.

The physical properties that govern the behaviour of the structure were calculated based on the structure's material properties and applied as strength parameters in components to tune the pathway analysis. For the axial stiffness of carbon rods, the $E \cdot A/L$ formula was used and resulted in carbon axial stiffness: 1.79MPa/m. For bending stiffness, the $E \cdot I$ formula was implemented, with Carbon rod bending stiffness: 699.5kPa/m² calculated. The pathway analysis results were cross-referenced with the behaviour observed in the physical models, confirming the validity of the pathway analysis (fig. 4(a-2)).

4.3 Generating the membrane

The membrane was generated separately from the pathway analysis because of notable difference in computational time between simulating the carbon rods as polylines and the closed mesh geometry, that represents the membrane. The structure is enveloped using a computational process known as the convex hull when the smallest convex set that includes all the points is created. This wrapping mesh serves as an initial approximation of the membrane. Afterwards, the generated mesh undergoes a reconstruction process using a component named 'tri-mesh'. This process is crucial as it unifies the mesh edge length, which is a key factor in the subsequent structural analysis (fig. 3(e)).

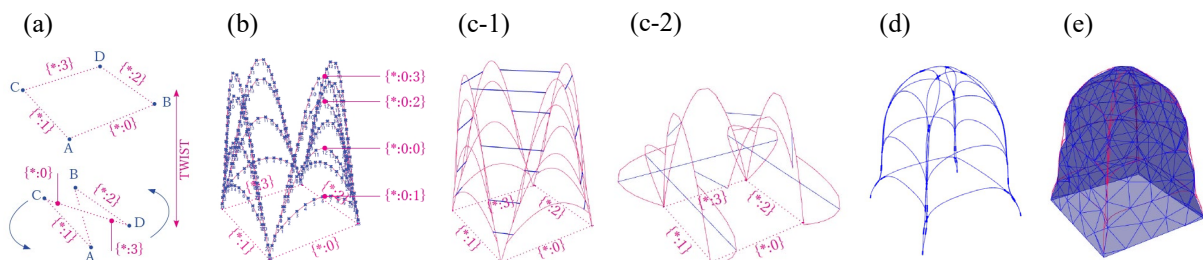


Figure 3: A – twisting base, B – generated skeleton, C – skeleton 1: maximum configuration, skeleton 2: configuration reflecting physical module, D – pathway analysis result, E – generated membrane.

4.4 Buckling analysis

The buckling analysis was implemented to check the structural integrity of the proposed structure. Analysis was conducted using a software stack that integrates Rhinoceros as the standalone CAD software, Grasshopper as an environment within Rhinoceros, and the ghHogan solver - the computational method that solves linear eigenvalue buckling analysis using the bisection method.

4.4.1 Linear EigenValue Buckling Analysis

A structure subjected to a load undergoes a series of deformations, the behaviour of which can be presented through its stiffness matrix. Solving this equation gives an eigenvalue of the system, which indicates the stability and performance of the structure.

The eigenvalue signifies the critical load factor at which a structural system may lose its stability. It serves as an approximation of the load at which buckling or other forms of instability might occur. An eigenvalue below 1.0 implies that the structure is unstable and will buckle under the applied loads. On the contrary, an eigenvalue greater than 1.0 indicates that the structure is stable and can withstand the applied loads without undergoing buckling. The eigenvalue can be used as a critical multiplier, indicating the load multiplier that is needed for critical failure. Eigenvalues can be particularly useful in detecting snap-through occurrences in multi-stable structures [17][18].

4.4.2. Analysis set-up

Material properties of the physical structure were converted to tf/m^3 units, suitable for structural analysis. Carbon Rods (CRP) were characterized by a Young's Modulus of $2.3265 \times 10^7 \text{tf/m}^2$, a Poisson's Ratio of 0.33333, and a density of 2.244898tf/m^3 . The organza material was defined by a Young's Modulus of 93877tf/m^2 , a Poisson's Ratio of 0.33333, and a density of 0.00002tf/m^3 . In terms of geometrical properties, the carbon rod elements have a cross-sectional area of 0.19635mm^2 , along with moments of inertia $I = 0.003068 \text{mm}^4$ and a torsional moment of inertia, denoted as $\text{VEN} = 0.006136 \text{mm}^4$. The organza elements feature a cross-sectional area of 1.1055mm^2 , moments of inertia $I_{xx} = 0.000147 \text{mm}^4$ and $I_{yy} = 70.368 \text{mm}^4$, and a torsional moment of inertia $\text{VEN} = 0.000589 \text{mm}^4$.

The load applied was the structure's self-weight. Due to the primary objective of ensuring the structural feasibility of the design, no external forces, such as those replicating outdoor conditions, including wind, were considered in the analysis at this stage. The focus was solely on understanding and optimizing the internal mechanics and stability of the structure, leaving the consideration of external environmental factors for future studies.

The analysis results were compared with the physical models to validate the computational findings (fig. 4 (a-3,4)). While analysing the skeleton without the organza membrane, the eigenvalue was found to be above 1, indicating that the structure is stable. However, the analysis of the skeleton with the organza membrane resulted in an eigenvalue below 1, indicating instability. The results correlate with the behaviour observed in the physical model - the skeleton could not withstand the weight of the organza and consequently collapsed.

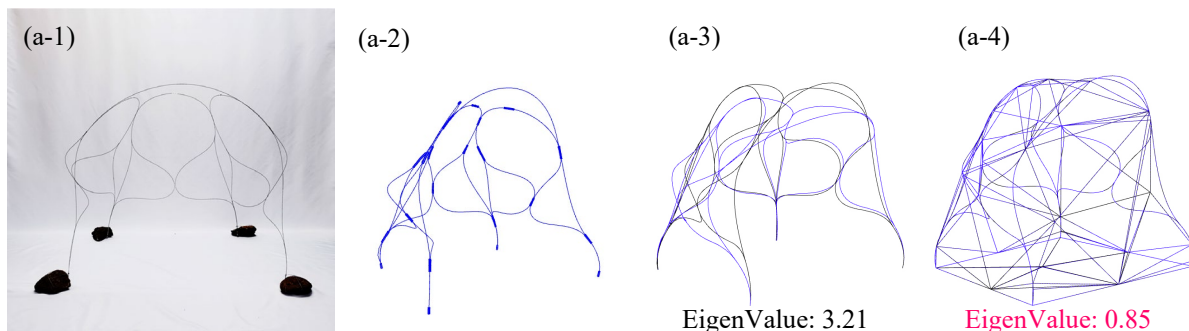


Figure 4: Buckling analysis result: 1 – physical model, 2 – pathway analysis result, 3 – only skeleton eigenvalue result, 4 – skeleton with membrane eigenvalue result.

4.5 Optimization

For the optimization process, the Galapagos plug-in is employed. This method utilizes an evolutionary solver, a form of artificial intelligence that mimics the process of natural selection, mutation, and crossover to find the most optimal solutions.

The optimization algorithm was provided with a set of 70 inputs: 68 integer values representing sliding joints and connectors on the structure and two floating-point values representing the x and y coordinates of the footprint. Depending on the values, joints could slide along the structure, changing where elements are buckled and where tension is applied. Furthermore, incorporating connectors allowed more freedom in the optimization process to create unique structures.

The optimization parameters were set to maintain a population of 50 solutions per generation. With each solution, the goal is to maximize the eigenvalue. On average, one iteration took approximately 25 seconds to converge using Razer Blade 15 advance model laptop with Intel(R) Core(TM) i7-10875H CPU, 16GB of RAM, and NVIDIA Ge-Force RTX 2080 Super Max-Q GPU.

5. Results

The optimization process was executed over 20 iterations, each consisting of 50 populations, resulting in a total of 1000 analysed models. Notably, the eigenvalue showed significant improvement during the optimization (fig. 5(a)). It increased from an initial value of 0.26061 to 1.825673 (fig. 5(b)) within the first 13 iterations. After this point, the eigenvalue remained stable, fluctuating within the same range.

Upon analysing the optimized model without the membrane, an eigenvalue of 0.639561 was recorded (fig. 5(c)). This suggests that the skeleton structure alone would not be stable enough to support its own weight, a result that was unexpected. The plausible explanation could be the role of the organza. In the physical model, the organza serves as an applied load that the skeleton must support. Therefore, in the buckling analysis, the geometry of the organza was included for a more realistic weight distribution. However, its structural behaviour was accounted for as well. As a result, the optimized structure could maintain stability only when tensioned by the membrane and was not self-supporting without it.

Based on the design principles established for this study, the structure needs to be free-standing to enable packing and deployment. Therefore, the optimization result could not be utilized as the end solution for the project. However, the optimization process did achieve its intended outcome: it successfully improved the eigenvalue of the skeleton when paired with the membrane, therefore the result was analysed to establish criteria, which resulted in improved structural performance.

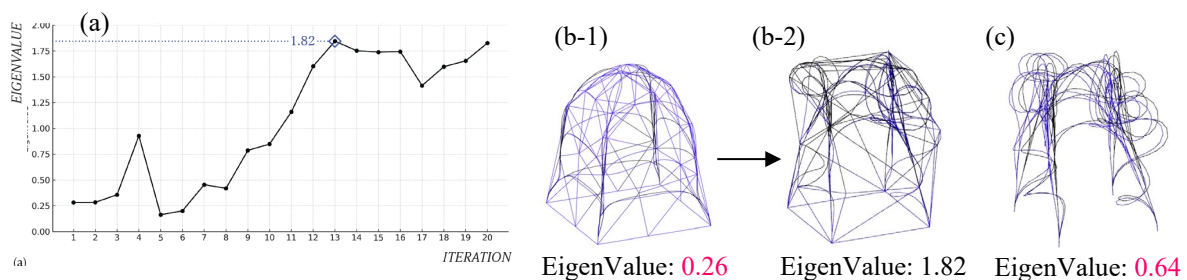


Figure 5: Optimization result: A – eigenvalue improvement, B – starting configuration (1) compared with optimized configuration (2), C – optimized skeleton without membrane.

5.1 Curly legs

Unlike the physical model, where elements typically branched at the base of the leg, the elements in the optimized model branched out elevated from the ground. Additionally, multiple elements—two to three—were bundled at a single point, a feature not present in the physical model. Of particular significance was the emergence of spiral and loop-like members, diverging from the straight or bent elements initially used in the design process. This unexpected geometric phenomenon was attributed to the close positioning of the sliding joints and connectors during optimization, which forced long elements to curl. This phenomenon can be linked to the fundamental property of rods, where any elastic rod can be held in a helical shape when equal and opposite forces are applied at the ends of the rod [19].

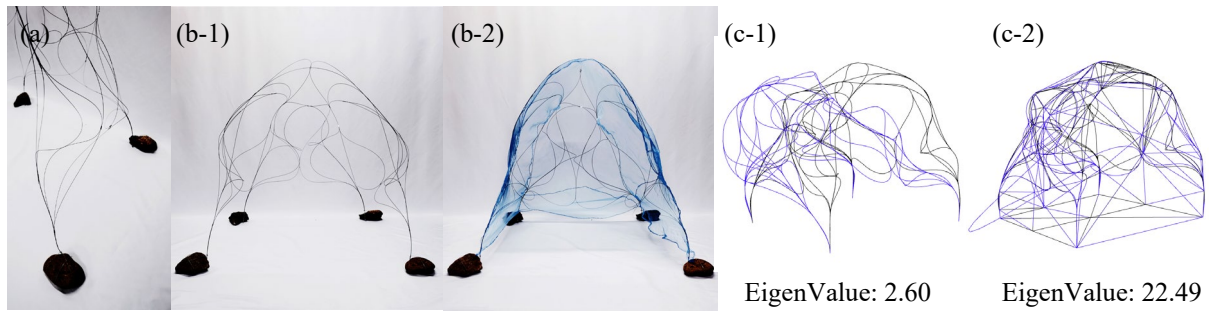


Figure 6: Improving the module: A – implementation of curly legs, B – improved skeleton (1) and improved skeleton with membrane (2), C – buckling analysis result of the skeleton (1) and skeleton with membrane (2).

The need for improvement in the physical module was addressed by applying insights observed from the optimization model. Utilizing physical prototyping, structural elements were added sequentially, adhering to principles identified during the optimization process. Specifically, elements branching near the base were incorporated. In addition, sliding joints were positioned closely to facilitate the curling of new structural elements, creating spirals that mirrored those in the optimized model (fig. 6(a)). After adding new features, which were termed “curly legs,” a noticeable increase in structural stiffness was observed (fig. 6(b-1)). This enhanced stability enabled the module to sustain the weight of the organza, thereby meeting the project’s structural requirements (fig. 6(b-2)).

Incorporating curly legs into the design aligned with the focus on using curved and bending-active geometries, and successful results only further proved the hypothesis of using stored elastic energy in buckled force-active elements in stiffening the structure (fig. 6(c-1,2)).

The final deployment process for the module could be finalized after the structure was improved. The process begins with the removal of the cap from the capsule (fig. 7(1)), thereby exposing the coiled rods and the tucked-in organza. After the organza is removed (fig. 7(2)), the protective sleeve is untied, enabling the gradual uncoiling of the skeleton structure (fig. 7(3)). Afterwards, the skeleton can be removed from the protective sleeve (fig. 7(4)), and the structure is ready for deployment.

Sliding the joints allows to elongate the structure to double its original length (fig. 7(5)). Subsequently, the structure is untwisted to establish its footprint and define the four legs (fig. 7(6)). Sliding joints are then moved to their marked positions to secure the form (fig. 7(7)). Following these steps, connectors are assembled to define the planes where snap-through will occur (fig. 7(8)). Legs are then installed sequentially to the footing (fig. 7(9)).

The final step involves placing the organza membrane over the skeleton (fig. 7(10)). This completes the deployment process, rendering the structure fully assembled.

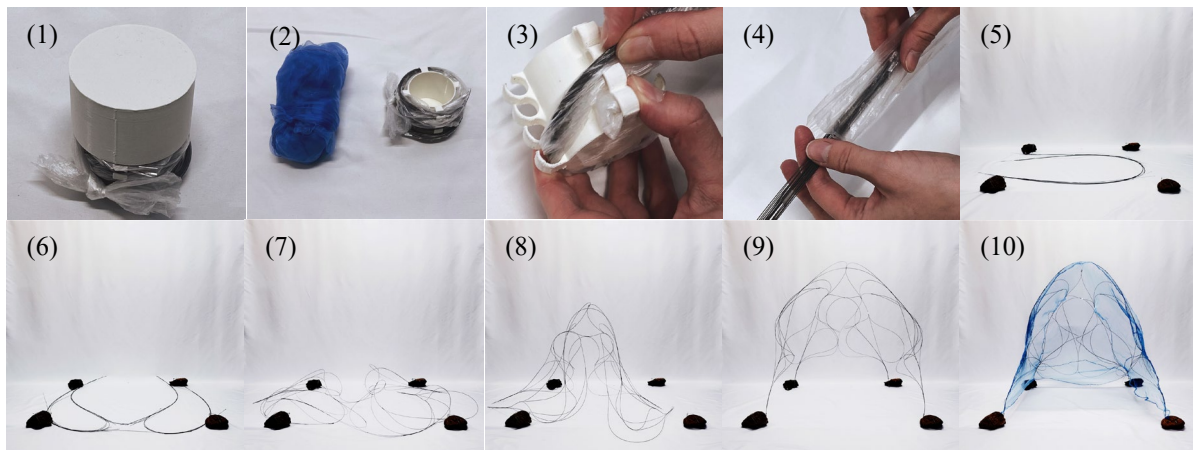


Figure 7: Deployment of the module

5.2 Gacha tent

After improving the snap-through module, three modules could be arranged together to create a modular tent that is named the “gacha tent” (fig. 8(a)). With deployed volume of $816,225 \text{ cm}^3$, the tent became a 3-gacha size structure, reducing the initially proposed deployment ratio to still an impressive 1570:1.

The gacha tent itself is remarkably lightweight. A total of 45 units of 3D-printed pieces are used, including 27 joints, 8 connectors, and 10 hooks, contributing to a total weight of 9 grams. The membrane, covering an area of 1.8 m^2 , also weighs 9 grams. The carbon rods contribute an additional 12 grams, bringing the total weight of a single module to 30 grams. For a tent composed of three such modules, the aggregate weight comes to a mere 90 grams (without capsules).

Building upon the background analysis of various tent options available in the market (fig. 8(b)), the Gacha tent takes ultra-compactness and lightweight design to a new level. However, it is essential to contextualize these achievements. The Gacha tent’s primary limitation is its suitability only for indoor environments, which differentiates it from the more robust outdoor tents. Furthermore, the tent’s deployment is relatively time-consuming due to its non-compliant sliding system and the requirement for manual tuning of the structure to reach stiffness. However, these issues should be seen as areas for improvement rather than inherent limitations, reinforcing the Gacha tent’s potential to become a feasible tent in the market.

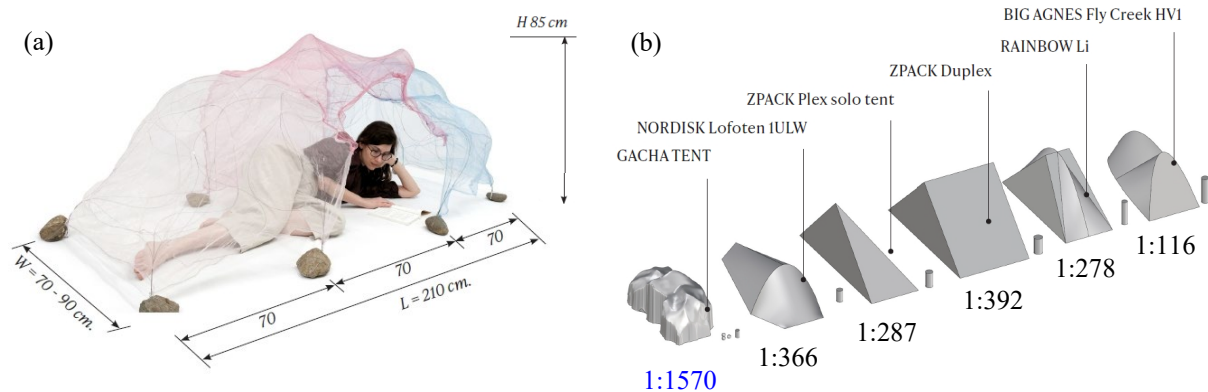


Figure 8: Gacha tent: A – Full configuration composed of 3 modules, B – Gacha tent deployment ratio compared with most compact tents in the market.

6. Conclusion

In this study, a design method was developed for implementing extremely slender structural members to meter-scale structures that can be compacted into a container in the size of a 7cm gacha capsule. The hypothesis that bend-active buckled elements could be used to increase the structure’s load-bearing capacity without increasing the mass of the materials was backed by the optimization results. By incorporating curly elements, the strength of the proposed structure could be increased, and an envisioned human-scale structure that can compress to a fraction of its size and fit in one pocket was achieved. However, working with extreme constraints did not come without limitations.

While the built structure has a high range of flexibility and can be animated with the slightest gust of wind without collapsing, it cannot withstand harsh outdoor conditions. However, while slightly increasing the diameter of the carbon rod, the strength of the structural members can be increased exponentially without a significant loss of strength-to-weight ratio. Additionally, the super organza, a material ill-suited to outdoor conditions, should be upgraded to waterproof material to use the tent in rainy conditions. With these adjustments more robust ultra-compact structures can be designed using the proposed method.

Achievements highlight the innovative approach of utilizing slender elements and lightweight materials to create an ultra-compact structure. The achieved high deployment rate pushes the boundaries in the field of compact structures. In conclusion, this study vitalizes the understanding of structure-force dynamics, presenting novel potentials for more efficient and elegant biomimetic deployable structures.

Acknowledgements

This research and development were financially supported by Tokyo-Princeton Fund.

References

- [1] “Eskimo Ice Fishing Gear,” Eskimo Ice Fishing Gear. <https://geteskimo.com/>
- [2] D. Melancon, B. Gorissen, C. J. García-Mora, C. Hoberman, and K. Bertoldi, “Multistable inflatable origami structures at the metre scale,” *Nature*, vol. 592, no. 7855, pp. 545–550, Apr. 2021.
- [3] Y. Yang, M. A. Dias, and D. P. Holmes, “Multistable Kirigami for Tunable Architected Materials,” *Phys. Rev. Materials*, vol. 2, no. 11, p. 110601, Nov. 2018
- [4] T. D. Ta, T. Umedachi, and Y. Kawahara, “A Multigait Stringy Robot with Bi-stable Soft-bodied Structures in Multiple Viscous Environments,” in *2020 IEEE/RSJ International Conference on Intelligent Robots and Systems (IROS)*, Oct. 2020.
- [5] T. Houette, E. Gjerde, and P. Gruber, “Unfolding Crease Patterns Inspired by Insect Wings and Variations of the Miura-ori with a Single Vein,” *Biomimetics*, vol. 4, no. 3, p. 45, Jul. 2019, doi: 10.3390/biomimetics4030045.
- [6] Y. Forterre, “Slow, fast and furious: understanding the physics of plant movements,” *Journal of Experimental Botany*, vol. 64, no. 15, pp. 4745–4760, Nov. 2013.
- [7] M. L. Smith, G. M. Yanega, and A. Ruina, “Elastic instability model of rapid beak closure in hummingbirds,” *Journal of Theoretical Biology*, vol. 282, no. 1, pp. 41–51, Aug. 2011.
- [8] Z. Wo and E. T. Filipov, “Stiffening multi-stable origami tubes by outward popping of creases,” *Extreme Mechanics Letters*, vol. 58, p. 101941, Jan. 2023.
- [9] Z. Zhai, Y. Wang, and H. Jiang, “Origami-inspired, on-demand deployable and collapsible mechanical metamaterials with tunable stiffness,” *Proceedings of the National Academy of Sciences*, vol. 115, no. 9, 2018,
- [10] A. Rafsanjani, K. Bertoldi, and A. R. Studart, “Programming soft robots with flexible mechanical metamaterials,” *Sci. Robot.*, vol. 4, no. 29, p. eaav7874, Apr. 2019.
- [11] B. S. Cox, R. M. J. Groh, D. Avitabile, and A. Pirrera, “Modal nudging in nonlinear elasticity: Tailoring the elastic post-buckling behaviour of engineering structures,” *Journal of the Mechanics and Physics of Solids*, vol. 116, pp. 135–149, Jul. 2018.
- [12] C. Gengnagel, H. Alpermann, and E. Hernández, *Active Bending in Hybrid Structures*. 2014.
- [13] T. Bessai, “Bending-Active Bundled Structures: Preliminary Research and Taxonomy Towards an Ultra-Light Weight Architecture of Differentiated Components,” presented at the ACADIA 2013: Adaptive Architecture, Cambridge (Ontario), Canada, 2013, pp. 293–300.
- [14] X. Zhang, R. Nie, Y. Chen, and B. He, “Deployable Structures: Structural Design and Static/Dynamic Analysis,” *J Elast*, vol. 146, no. 2, pp. 199–235, Nov. 2021.
- [15] “Deployable Structures,” MMA Design LLC. <https://mmadesignllc.com/products/deployables/>.
- [16] S. Pellegrino, Ed., *Deployable Structures*. Vienna: Springer Vienna, 2001.
- [17] H. Ujioka, K. Isebo, S. Kazaoui, and J. Sato, “Deployable polyhedral structure with snap-through behavior induced by dimples on metal panels,” *Proceedings of IASS Annual Symposia*, vol. 2022, no. 14, pp. 1–12, Sep. 2022.
- [18] R. Stankeviciute and J. Sato, “Snap-through buckling detection and analysis method for multi-stable structures,” *Proceedings of IASS Annual Symposia*, vol. 2023, pp. 2610-2619, Sep. 2023.
- [19] A. E. H. Love, *A treatise on the mathematical theory of elasticity*, 4th ed. New York: Dover Publications, 1944.